A review of angle domain common image gathers

Faranak Mahmoudian and Gary F. Margrave

ABSTRACT

Common image gathers in the offset domain are used extensively in velocity analysis and amplitude versus offset (AVO) studies. Imaged with the correct background velocity model, the events will appear horizontal in the seismic offset gathers. Any curvature or moveout in these gathers can be used as a criterion for updating migration velocities. If the geology is complex and the ray field becomes multi-pathed, then the assumptions made for imaging data in the offset domain are violated. This will especially influence the quality of common-image gathers and, as a sequence, make it difficult to perform any form of AVO or velocity analysis. Such complicated problems typically arise in seismic imaging beneath gas, salt domes, and basalt structures. Angle-domain common image gathers (ADCIGs) uniquely define ray couples for each point in the subsurface. Therefore, each event in the data will be associated with only one subsurface location. It is possible to generate the ADCIGs with both Kirchhoff and wave-equation migration methods, these ADCIGs may be used for velocity analysis and amplitude-versus-angle (AVA) analysis. Common-angle migration creates seismic images for different reflection angles at the reflector, thus generating ADCIGs. The ADCIGs may be used for velocity analysis, and amplitude versus angle (AVA) analysis with the specific application in a fracture study. AVA can provide information about fractures at existing wells, in reservoir characterization specially in predicting the production rates of new wells, and in structural interpretation. Since AVA records the fracture information between the wells, it adds significant information to the interpretation of fractured reservoirs that cannot be easily obtained in other ways.

Discussing common-angle migration, a summary of the Kirchhoff-based method as based on the work of Bleistein et al. (2001) is presented. In addition, the wave-equation-migration based method, which is discussed in the work by Sava (2001), is examined. Further, a brief review of the application of ADCIGs in amplitude-versus-angle and azimuth (AVAZ) analysis by Gray et al. (2002) is presented.

1. INTRODUCTION

Common image gathers (CIGs) provided by common-offset or common-shot migrated data are commonly used for migration-based velocity analysis (Symes, 1993) and AVO analysis (Beydoun et al., 1993 and Tura et al. 1998). Since the most relevant information for velocity analysis or AVO studies is not described by zero-offset images, the study of offset domain common image gathers (ODCIGs) is widely employed. The ODCIGs can be produced by Kirchhoff migration methods, or by wave-equation migration methods. For a perfectly known velocity model, the ODCIGs generated by Kirchhoff migration produce flat events, whereas the ODCIGs generated by wave-equation migration produce events perfectly focused at zero offset. For the complex geology, the ODCIGs are affected by artefacts, and their quality deteriorates. Xu et al. (2001) showed that for complex velocity models, ODCIGs can be strongly affected by artefacts, even when a correct velocity model is used for the migration. As described by Xu et al. (2001), it may be observed in the 2D Marmousi dataset that for the exact velocity, the ODCIGs

generated by Kirchhoff migration were not flat, although the migration stack was satisfactory (Duquet, 1996). One potential cause of the artefacts on ODCIGs is reflector ambiguity due to multi-pathing of reflected energy. Multi-pathing occurs in geologically complex situations, such as imaging beneath gas clouds, salt bodies, and basalt formations, in which the single path assumption (made by most of the methods generating the ODCIGs) is violated (Ursin, 2004). Several authors have suggested angle domain imaging as a solution for multi-pathing (de Hoop et al., 1994; Brandsberg-Dahl et al., 1999; Prucha et al., 1999; Xu et al., 2001 and Bleistein and Gray, 2002).

An ADCIG collects the energy in a data set which has been scattered over a specific reflection ("opening[1]") angle. This opening angle is the angle between the source and receiver rays at an image point, shown schematically in Figure 1. Unlike ODCIGs, ADCIGs produced with either kind of migration method are flat since they simply describe the reflectivity as a function of incident angle at the reflector (Sava and Fomel, 2003), as in Figure (2). The ADCIGs can be produced during or after the migration process. The ADCIGs uniquely define ray couples for each point in the subsurface; therefore each event in the data will be associated with only one subsurface location. To describe the kinematics of multi-pathing and the capability of an ADCIG to separate the multi-pathed rays, the two following 2D models are considered.

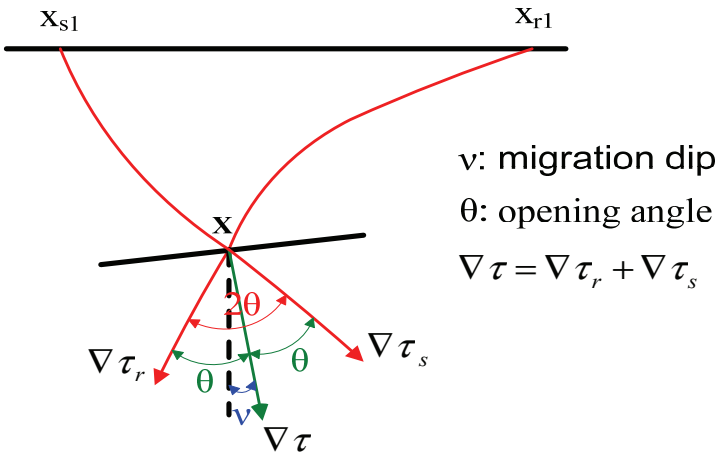

FIG. 1. Angles in common-angle Kirchhoff M/I. 2θ is the opening angle between the source and receiver ray. Migration dip ***v*** is the angle between the direction of sum of the gradient of travel-times from source and receiver, and the vertical axis. The angles between source-ray or receiver-ray and migration dip direction is half of opening angle (This is only true for an isotropic background medium).

Model one: Described by Bleistein and Gray (2002), assume a single subsurface point with several multiple specular ray pairs, as depicted in Figure (3). A specular point is an image point which the sum of ray vectors from the source and receiver to that point, aligns with the normal to the surface at that point; that is when an image of the reflector at that point is expected. When multiple arrivals from a subsurface location occur, the migration output is a sum over two or more specular ray couples. As illustrated in Figure (3), for one subsurface point the multiple specular rays have the same offset, but different

[1] For acoustic case reflection angle is half of the opening angle.

opening angles. A common-offset migration/inversion (M/I) that uses only one arrival will pick up a contribution from only one of these specular rays; while a common-offset M/I that uses multiple passes to pick up all returns, will add all arrivals. Therefore for such subsurface points the common-offset M/I will always make amplitude studies problematic. As illustrated in Figure (3), common-offset traces which have more than one specular source-receiver pair, the opening angle for these different specular events will be different; so when they are placed into different common-angle panels, no summing of contributions from different specular arrivals occurs. Hence, an ADCIG is a wise approach for dealing multi-pathing in this case.

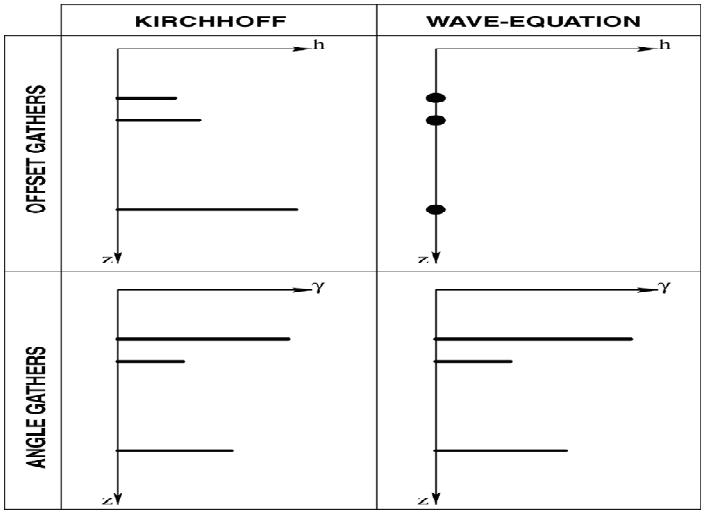

FIG. 2. Offset domain and angle domain common image gathers. A schematic comparison between Kirchhoff and wave-equation methods (Sava and Fomel, 2003).

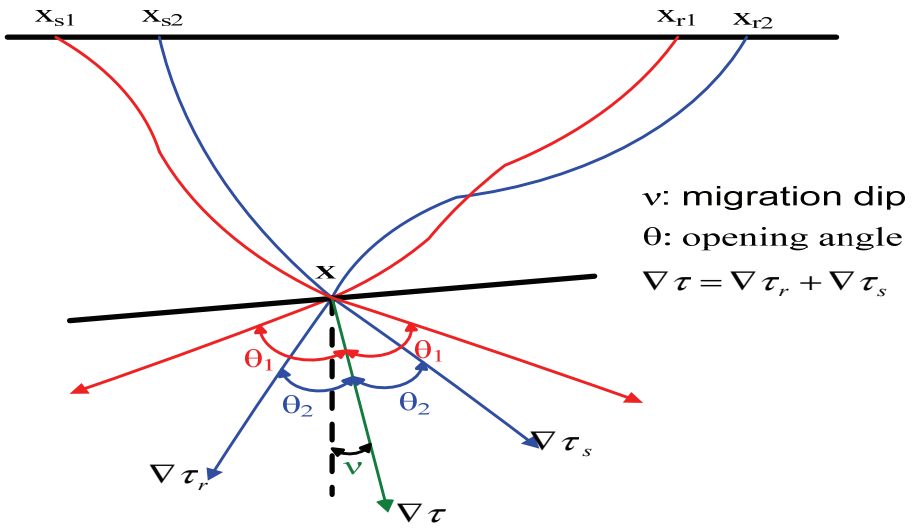

FIG. 3. A dipping reflector with two sets of specular rays that have the same offset but different opening angles at depth.

Model two: If two raypaths between the same source and receiver exist such that they have the same receiver horizontal slowness and the two-way travel-time along each is the same, it is impossible to distinguish between the two reflector locations (Nolan and Symes, 1996), as shown in Figure (4). Another case of multi-pathing described by Prucha et al., (1999), a common shot gather or common offset gather that contains two events from two points in the subsurface that arrive at the same time. As illustrated in Figure (5), the circular lens is a low-velocity anomaly in a constant velocity surrounding. Both subsurface points (X and Y) have the same mid-point and migration dip angle (the same horizontal midpoint slowness) but different opening angle Once again, the two ray paths represent the same event and the location of the reflector causing this event is completely ambiguous in an ODCIG; whereas these two raypaths would be mapped into different angles of an ADCIG.

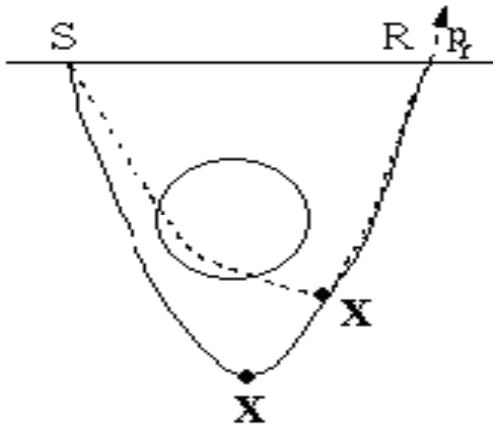

Fig. 4. Individual shot gather: the circular lens is a low velocity anomaly, so the traveltimes and p_r are identical (Nolan and Symes, 1996).

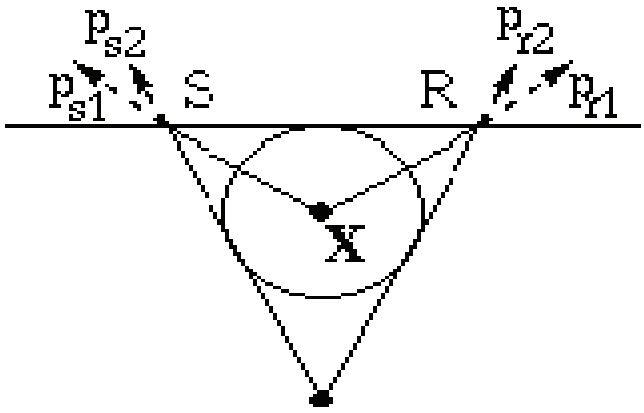

FIG. 5. An individual offset gather: the circular lens is a low velocity anomaly, so the travel-times are identical and the midpoint slownesses are equal (Prucha et al. 1999).

This paper starts with a brief description of methods that generate ADCIGs for elastic and acoustic cases. Then, for acoustic case, the paper continues with a summary of the common angle migration using the M/I method described in Bleistein and Gray (2002),

Bleistein et al., (2005); Zhang et al., (2007)[2]. This is followed by a summary of generating ADCIGs using wave-equation migration methods (Prucha et al., 1999; Fomel and Prucha, 1999; Sava and Fomel, 2003 and Fomel, 2004). Finally, a brief overview of the application of ADCIGs in fracture studies is presented.

2. ELASTIC CASE

For the most general anisotropic elastic case, the ADCIGs have been generated using the common-angle migration-inversion method. Common-angle M/I proposed by de Hoop and his collaborators requires implementation of the Generalized Radon Transform (GRT) techniques and an understanding of pseudo-differential operators; de Hoop and Bradsberg-Dahl (2000) extended the GRT technique to account for the caustics effect and the multipathing related to that, using Maslov theory. A tutorial on common-angle M/I using GRT in anisotropic elastic media is available by Ursin (2004). Sollid and Ursin (2003) applied the common-angle M/I of de Hoop and Bradsberg-Dahl to an ocean-bottom seismic data assuming weak anisotropy. They were able to construct a well-focused PP image of a studied reservoir which was located directly beneath a gas cloud in the overburden. Figure (6) shows the Sollid and Ursin's PP common-image gathers from the reservoir zone generated by a conventional common-offset migration (top) and a common-angle migration (bottom); the improvement in signal-to-noise ratio seen in the ADCIG indicating the capability of common-angle migration in handling the multi-pathing problem.

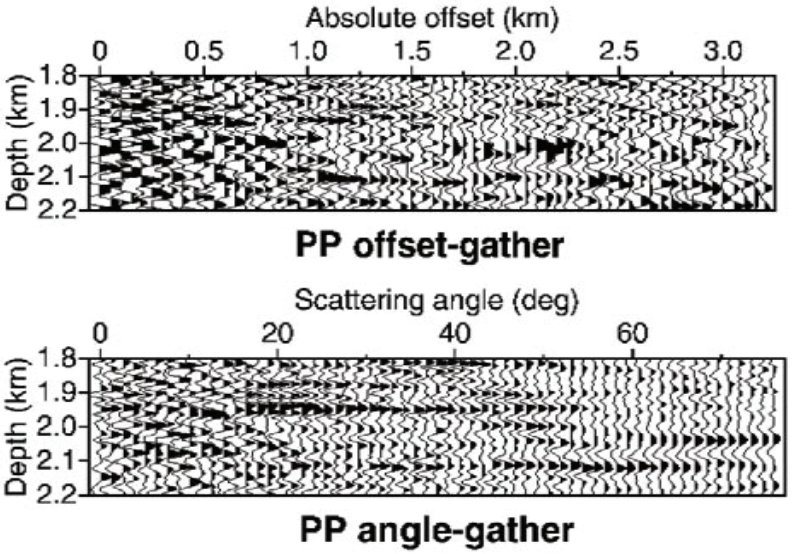

FIG. 6. Comparison between common-offset and common-angle migration of ocean-bottom seismic data (Sollid and Ursin, 2003).

[2] They used the same coordinate transform (converting subsurface coordinates to surface coordinates) as Bleistein et al. (2005), in their wavefield extrapolation migration.

3. ACOUSTIC CASE

3.1 KIRCHHOFF RAY-BASED METHODS

De Hoop and Brandesberg-Dahl (2000) presented formulae for the most general anisotropic elastic case, from which it is difficult to determine results for simpler cases (Bleistein and Gray, 2002). For the acoustic case, Xu et al. (2001) presented an analysis of multi-pathing artefacts through the study of the ray-based M/I operator. They proposed working in the angle domain for unfolding multi-pathed ray fields. They discussed that sorting into angle gathers cannot be done as a prior over the dataset, but is done in the inner depth migration loop. Xu et al., (2001) presented a two-dimensional (2D) Kirchhoff inversion formula as an integral of input reflection data over all possible migration dip angles at an image point for each fixed value of the opening angle between the rays from the source and receiver at an image point (see Figure (1) for a definition of migration dip and opening angle). Then they recast the result as an integral over source and receiver points on the acquisition surface. To test the capability of the method in imaging of complex media, Xu et al. (2001) applied the common-angle M/I to the Marmousi dataset. Figure (7) compares their CIGs in shot, offset and angle domains for two locations, one in the non-complex part and one in the complex part of the Marmousi model. Common angle migration results are incomparably better than those obtained with common-shot or common offset M/I. Figure (8) shows a common shot, common offset, and common angle image over the full target; strong artefacts appear in the common shot and common offset images, much better results are obtained for the common angle image.

For the acoustic case, Bleistein and Gray (2002) also proposed a 3D common-angle M/I. Their 2D version formula is equivalent to formula derived by Xu et al. (2001). Their derivation arises from the more classical method, the Kirchhoff M/I technique as described in Bleistein et al., (2001).

3.1.1 COMMON-OPENING ANGLE MIGRATION/INVERSION

This section summarizes the work of Bleistein et al., (2002-2005) on common opening angle M/I for the acoustic medium. They derived a Kirchhoff M/I technique as an integral over migration dip at an output point at depth; compared to common shot or common offset that are integrals over surface coordinates. The common angle M/I method is an alternative Kirchhoff method for a different sorting of the data. The derivation arises from a more classical Kirchhoff modeling and inversion theory (Bleistein et al., 2001) more accessible to the geophysical community.

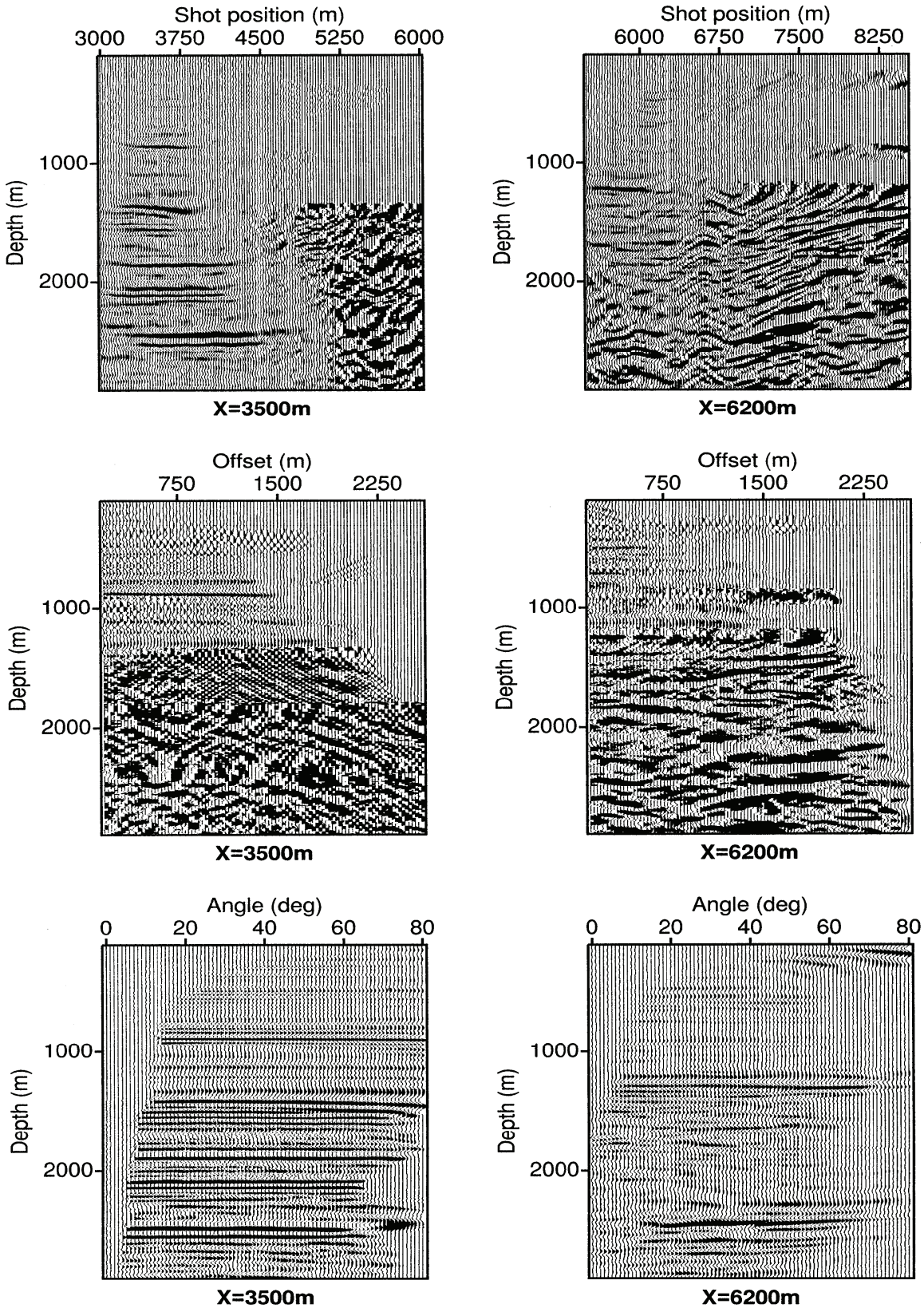

FIG. 7. CIGs in shot, offset, and angle in the noncomplex (X =3500 m) part and in the complex (X =6200 m) part of the Marmousi model. Results are displayed in relative impedance perturbation and are plotted with the same clip (Xu et al., 2001).

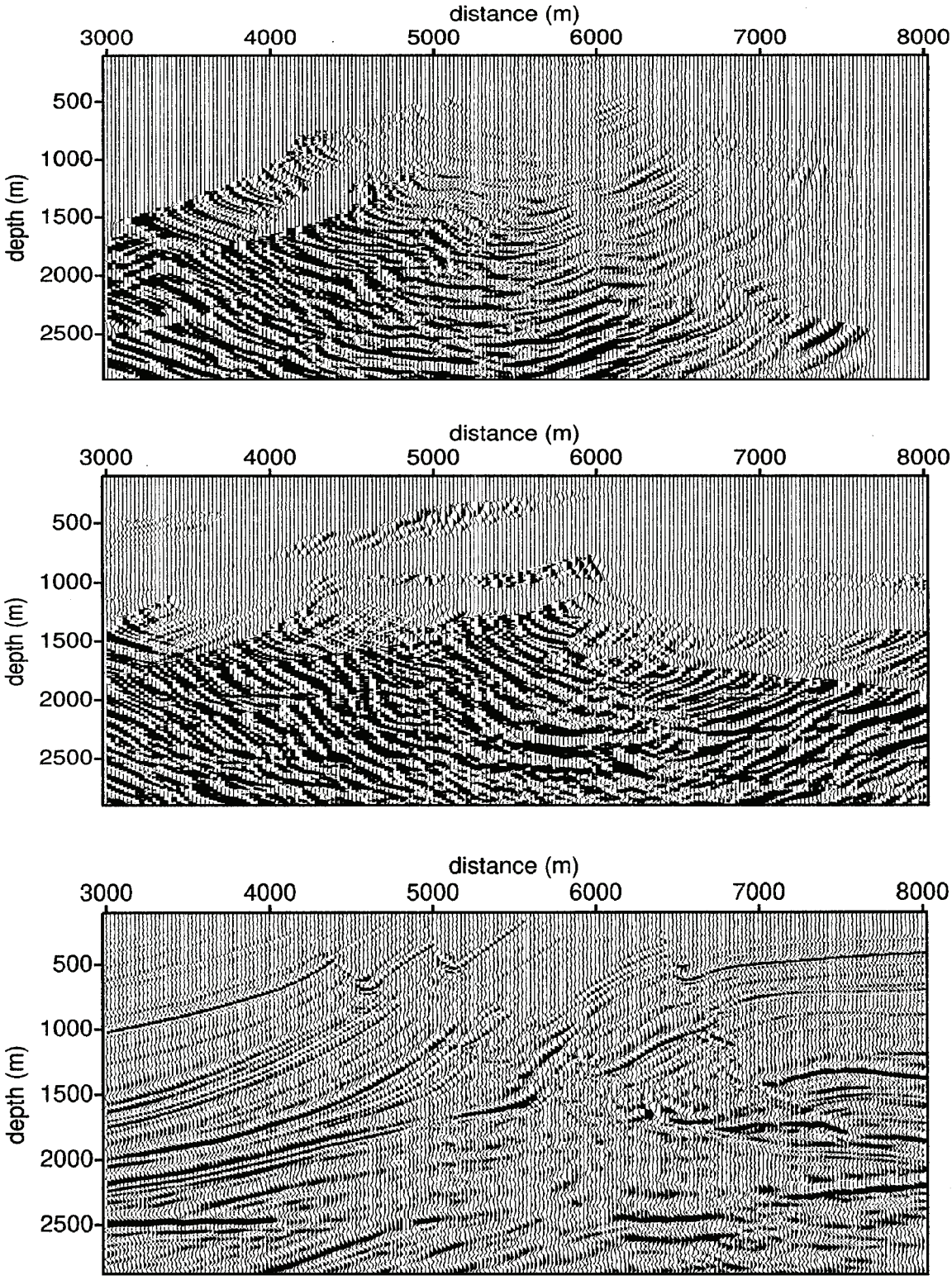

FIG. 8. (Top) Common-shot image panel for shot X= 6000 m. (Middle) Common-offset panel for offset h= 950. (Bottom) common-angle panel for angle theta= 45. Results are clipped to the exact value of the image (Xu et al., 2001).

A very short summary of the Kirchhoff M/I method of Bleistein et al. (2001) is as follows. They formulated the inverse problem by writing a forward modeling formula that was an integral equation for the scattered field. By linearizing this integral equation via the Born approximation and by substituting the high-frequency approximation of constant-wavespeed Green's function, the resulting integral had the form of a Fourier transform. Therefore, the inverse formula was written as an inverse Fourier transform (valid asymptotically). Their initial formalism yielded a solution for the wavespeed perturbation from some assumed background value. They then they modified the results to invert for the reflectivity function. To perform beyond the constraints imposed by the Born approximation, they applied the Fourier inversion operator to Kirchhoff-approximate[3] data, yields asymptotically the reflectivity function.

The starting point for derivation of common-opening angle M/I is proposing an inverse formula based on the Kirchhoff-approximate data. Kirchhoff-approximate data is an approximation of upward scattered field response from a single reflector. The mathematical detail of this derivation is on appendix A. The reflectivity function from this common opening angle M/I for fixed opening angle θ and azimuth φ is

$$R(x)\big|_{\text{fixed }\theta\text{ and }\varphi} = \frac{1}{4\pi^2}\frac{2\cos\theta}{c(x)}\int \frac{D(x,x_s,x_r)}{A(x,x_s)A(x,x_r)}\sin\alpha_1 d\alpha_1 d\alpha_2, \qquad (1)$$

where x is the subsurface point, θ is half of opening angle, $c(x)$ in the velocity at point x, α_1 and α_2 are two parameters that defines migration dip at point x. $\boldsymbol{D}$ is a filtered version of input traces $u(x,x_s,x_r)$ as

$$D(x,x_s,x_r) = \frac{1}{2\pi}\int iw\, u(x,x_s,x_r)\, \mathrm{e}^{-iw\tau(x)} dw, \qquad (2)$$

with $\nabla\tau$ is the gradient of the sum of the travel times from the source and receiver to the subsurface point x (as indicated in Figure (1)). To compute the M/I integral of equation (1) in a practical sence, the integral should be recast as an integral over the source and receiver points. Equation (1) is a function of two parameters while an integral over source and receiver points will be over four variables. To get around this one can do this trick, rewriting the right hand side of equation (2) as an integral in the four variables, $\alpha_1, \alpha_2, \theta' and\ \varphi'$ as follows:

$$\begin{aligned} R(x) &= \frac{1}{4\pi^2}\int \frac{2\cos\theta'}{c(x)}\frac{D(x,x_s,x_r)}{A(x,x_s)A(x,x_r)}\sin\alpha_1\delta(\theta-\theta')\delta(\varphi-\varphi')d\alpha_1 d\alpha_2 d\theta' d\varphi' \\ &= \frac{1}{4\pi^2}\int \frac{2\cos\theta'}{c(x)}\frac{D(x,x_s,x_r)}{A(x,x_s)A(x,x_r)}\sin\alpha_1\delta(\theta-\theta') \times \\ &\quad \sin\theta'\,\delta\left(\sin\theta'(\varphi-\varphi')\right)d\alpha_1 d\alpha_2 d\theta' d\varphi' \end{aligned} \qquad (3)$$

This enables to restrict the input traces to those with the fixed common-opening angle and azimuth. Here the Dirac delta-functions provide a device which the integral in two

[3] Derivation of Kirchhoff approximated data is available at appendix (E) of Bleistein et al., (2001).

variables is recast as an integral in four variables. Now we need to transfer these variables $\alpha_1, \alpha_1, \theta', \varphi'$ to surface variables $x_{s1}, x_{s2}, x_{r1}, x_{r2}$ using the Jacobian. Bleistein et al., (2005) derived this transform as:

$$\begin{aligned}\sin\alpha_1 d\alpha_1 d\alpha_2 d\theta' d\varphi' &= \frac{\partial(\alpha_1,\alpha_2,\theta',\varphi')}{\partial(x_{s1},x_{s2},x_{r1},x_{r2})} dx_{s1}dx_{s2}dx_{r1}dx_{r2} \\ &= \left[16\pi^2\right]^2 \frac{\cos\beta_s}{v(x_s)}\frac{\cos\beta_r}{v(x_r)}\frac{c^2(x)}{2\sin 2\theta'} A^2(x,x_s)A^2(x,x_r)dx_{s1}dx_{s2}dx_{r1}dx_{r2}\end{aligned} \tag{4}$$

where, the angles β_s and β_r are emergence angles at source and receiver, $v(x_s)$ and $v(x_r)$ are velocity at source and receiver, $A(x_s)$ and $A(x_s)$ are Green function amplitudes. The transform in (4) makes the inversion formula in **Error! Reference source not found.** become:

$$\begin{aligned}R(x) = 32\pi^2 c(x)\int \frac{\cos\beta_s}{v(x_s)}\frac{\cos\beta_r}{v(x_r)} D(x,x_s,x_r)A(x,x_s)A(x,x_r) \\ \delta(\theta-\theta')\delta(\theta'-\theta)\delta\left(\sin\theta'(\varphi-\varphi')\right)dx_{s1}dx_{s2}dx_{r1}dx_{r2}.\end{aligned} \tag{5}$$

In practice, this integral will be carried out discretely. Rreplace the discrete approximations of Dirac function as follows:

$$\begin{aligned}\delta(\theta-\theta') &\approx \begin{cases}\dfrac{1}{\Delta\theta}, & \theta-\dfrac{\Delta\theta}{2}\le\theta'\le\theta+\dfrac{\Delta\theta}{2} \\ 0, & otherwise.\end{cases} \\ \delta(\sin\theta'(\varphi-\varphi')) &\approx \begin{cases}\dfrac{1}{\sin\theta'\Delta\theta}, & \theta-\dfrac{\Delta\varphi}{2}\le\theta'\le\theta+\dfrac{\Delta\varphi}{2} \\ 0, & otherwise.\end{cases}\end{aligned} \tag{6}$$

Then the discrete version of equation (5) for the reflectivity function as an integral over all sources and receivers is

$$R(x) = \frac{32\pi^2 c(x)}{\sin\theta\Delta\theta\Delta\varphi}\int \frac{\cos\beta_s}{v(x_s)}\frac{\cos\beta_r}{v(x_r)} D(x,x_s,x_r)A(x,x_s)A(x,x_r)dx_{s1}dx_{s2}dx_{r1}dx_{r2}. \tag{7}$$

Bleistein et al. (2005) suggested M/I formula (7) to calculate 3D ADCIG at reflection angle θ from data at azimuth φ. In summary, starting from a Kirchhoff M/I formula as an integral in migration dip direction coordinates at an image point, a Kirchhoff M/I as an integral over all sources and receivers at the upper surface is derived; that is, over all data traces.

It wouldn't be fair to finish the review of Kirchhoff methods in generating ADCIGs, without mentioning an argue by Stolk and Symes (2002). Stolk and Symes (2002) argue that even in perfectly known but strongly refracting media, Kirchhoff ADCIGs are

hampered by significant artefacts caused by the asymptotic assumptions of ray-based imaging. They presented a common framework for understanding the presence or absence of image artefacts in both offset and angle-domain Kirchhoff migration and claim that the formulation of Kirchhoff migration in the common-angle domain does not suppress imaging artefacts, contrary to assertions in the literature (Xu et al., 2001). They doubt the Xu et al., (2001) assert that common-angle pre-stack Kirchhoff depth migration does not produce image artefacts; arguing that the examples presented in (Xu et al., 2001) are too complex to convincingly support such a conclusion, nor could a few examples in themselves establish such a categorical assertion.

3.2 WAVE-EQUATION MIGARTION METHODS

This section focuses on ADCIGs computed in relation with wave-equation migration. Several authors have produced ADCIGs using wave-equation migration among de Bruin et al. (1990), Prucha et al. (1999), Mosher and Foster (2000), Sava and Fomel (2003), Zhang et al. (2007). There are two possible approaches to angle-gather construction with wavefield continuation. In the first approach, one generates gathers at each depth level converting offset-space frequency planes into angle-space planes simultaneously with applying the imaging condition (Prucha et al., 1999); this method generates angle gathers during migration, called *data-space* method. In the second approach, one converts migrated images in offset-depth domain to angle-depth gathers after imaging of all depth levels is completed (Sava and Fomel, 2003); this method generates angle-gathers after and not during migration, called *image-space* method. Following section will review these two methods briefly.

3.2.1 DATA-SCAPE METHOD

This section summarizes the work of Prucha et al. (1999) on extracting ADCIGs from downward continued pre-stack data. Consider a 3D seismic data organized as a function of midpoint coordinates (***m***) and offset coordinates (***h***). Prestack data are efficiently downward continued using the double-square-root (DSR) equation in the frequency domain. Furthermore, since they either use 2D downward continuation or 3D common-azimuth downward continuation, the offset space is restricted to the in-line offset h_x, thus we express the recorded wavefield as $P(w, m, h_x; z = 0)$, where z is depth and $z = 0$ indicates data recorded at the surface.

The pre-stack wavefield at depth is obtained by downward continuing the recorded surface data using the DSR method, and is imaged by extracting the values at zero time. The usual migration process can be represented schematically as

$$P(w, m, h_x; z = 0) \xrightarrow{DSR} P(w, m, h_x; z) \tag{8}$$

$$P(w, m, h_x; z) \xrightarrow{imaging} P(t = 0, m, h_x; z). \tag{9}$$

The downward-continuation process focuses the wavefield towards zero offset and if the continuation velocity is correct, a migrated image can be obtained by extracting the

value of the wavefield at zero-offset. Therefore, to obtain ODCIGs an extra step is needed. A slant stack is performed along the offset axis before imaging, and then an image as a function of the offset ray parameter will be obtained. The migration process used to produce ODCIGs can be represented schematically as

$$P\left(w,m,h_x;z=0\right) \xrightarrow{DSR} P(w,m,h_x;z) \tag{10}$$

$$P\left(w,m,h_x;z\right) \xrightarrow{Slant\ stack} P(\tau,m,p_{hx};z) \tag{11}$$

$$P\left(\tau,m,p_{hx};z\right) \xrightarrow{Imaging} P(\tau=0,m,p_{hx};z) \tag{12}$$

Angle-domain CIGs are subsets of at fixed midpoint locations. Strictly speaking, the CIG gathers obtained by the proposed procedure are functions of the offset ray parameters and not of the reflection angle. However, is linked to reflection angle, γ, by the following simple trigonometric relationship

$$\frac{\partial t}{\partial h} = p_{hx} = \frac{2sin\gamma cos\alpha}{v(z,m)}, \tag{13}$$

where α is the geological dip along the in-line direction and is the velocity function; a simple proof illustrated in Figure (9). The right panel in Figure (10) shows the ADCIG corresponding to the downward-continued offset gather shown in the left panel.

As mentioned in the introduction, the ADCIGs can be use for wave-equation migration velocity analysis; if the velocity function is correct the reflections are aligned along the angle axis. If the velocity is too low the reflections will smile upward (Figure 11); if the velocity is too high the reflections will from frown downward.

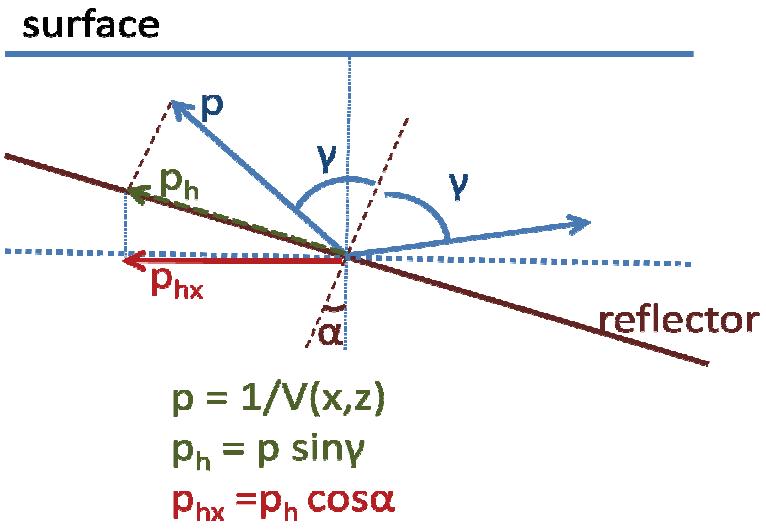

FIG. 9. A simple trigonometric proof for equation (13).

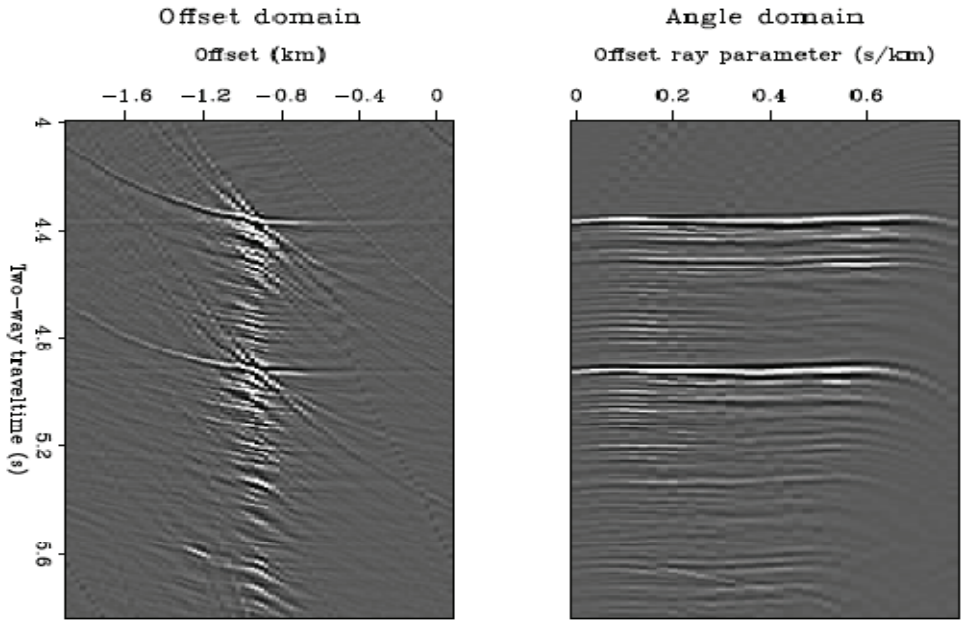

FIG. 10. (Left): Offset-gather CIG after downward continuation. (Right): Angle-domain CIG (Prucha et al., 1999).

In practice, computing ADCIGs before imaging for wave-equation migration is computationally demanding (Biondi, 2007). Therefore, ADCIGs rarely computed before imaging, when using shot-profile migration. In the upcoming section, we will see how computing ADCIGs after imaging addresses this problem.

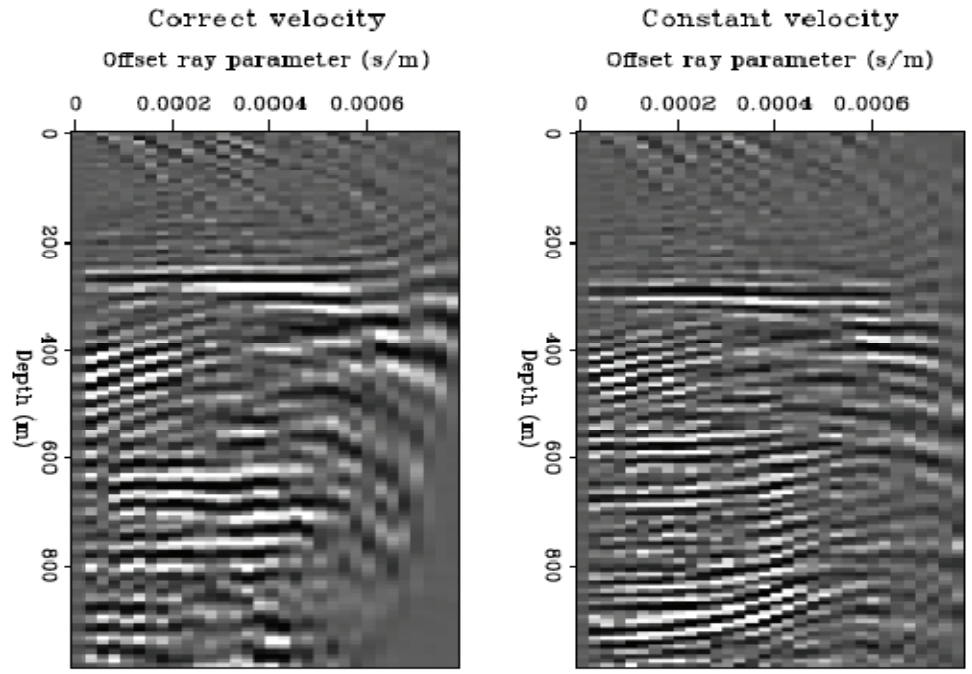

FIG. 11.(Left): ADCIG with correct velocity. (Right): ADVIG with too low constant velocity (Prucha et al., 1999).

3.2.2 IMAGE-SPACE METHOD

This section summarizes the work of Sava and Fomel (2003) on extracting angle gathers from migrated images. This method operates on prestack migrated images and produces the output as a function of reflection angle, not as a function of offset ray parameter as in data-space method.

Sava and Fomel (2003) suggest a simple Radon-transform procedure for Angle-gathers can be conveniently formed in the frequency-wavenumber domain using wavefield continuation methods. Consider equation (13), we can also write

$$\frac{\partial t}{\partial z} = p_z = \frac{2\cos\gamma\, cos\alpha}{v(z,m)}. \tag{14}$$

From equations (13) and (14), we can write

$$tan\gamma = -\left.\frac{\partial z}{\partial h}\right|_{t,x}, \tag{15}$$

the relation which is the basis for generating an angle-gather. Equation (15) is derived for a constant velocity media, but it remains perfectly valid in a differential sense in any arbitrary velocity media if we consider $\boldsymbol{h}$ to be half the offset at the reflector depth. The full derivation of equation (15) is available in appendix A of Sava and Fomel (2003) paper. In the frequency-wavenumber domain, formula (15) takes the simple form

$$tan\gamma = -\frac{k_h}{k_z}, \tag{16}$$

where k_z ($k_z = wp_z$) and k_h($k_h = wp_h$) are the depth and offset wavenumber, respectively. Equation (16) indicates that ADCIGs can be formed using frequency-domain algorithms.

The introduced angle-gather transformation amounts to a stretch of the offset to a reflection angle according to equation (16). The stretch takes every point on the offset wavenumber axis and repositions it on the angle axis, most likely not on its regular grid. Therefore, there is a need to interpolate the unevenly sampled axis to the regular one after an angle-gather transform.

3.2.3 IMAGE-SPACE METHOD VERSUS DATA-SPACE METHOD

As described in Sava and Fomel (2003), the major differences between data-space and image-space methods in calculating ADCIGs from wave-equation migration are the following:

1. The image-space method is completely decoupled from migration. Therefore, conversion to reflection angle can be thought of as a post processing step after migration. Such post processing is useful because it allows to shuttle between angle and offset domains without remigrating the data. This conclusion which does not hold true for the data-space method, where the transformation is a function of the data frequency.

2. The angles we obtain using equation (16) are geometrical measures of the reflection angle. For amplitude variation with angle (AVA) purposes, it is convenient to have the reflected amplitudes described as a function of reflection angle and not as a function of offset ray parameter, a case in which conversion to reflection angle requires reflection dip and velocity information, as in equation (13).
3. Both ADCIGs methods require accurate knowledge of the imaging velocity. The difference is that the data-space method is less sensitive to inaccuracies in the location of sharp velocity boundaries because the conversion to angle-gathers is done at every step as the wavefield is continued in depth. In contrast, the image-space angle gathers are created using the information contained in the entire image gathers. Therefore slight imaging errors at a given depth influence angle gathers at other depth levels. However, conversion from p_{hx} to the reflection angle γ is influenced by errors in the velocity maps as well.

Figure (12) show the different amplitude behaviour between the image space and data space methods:

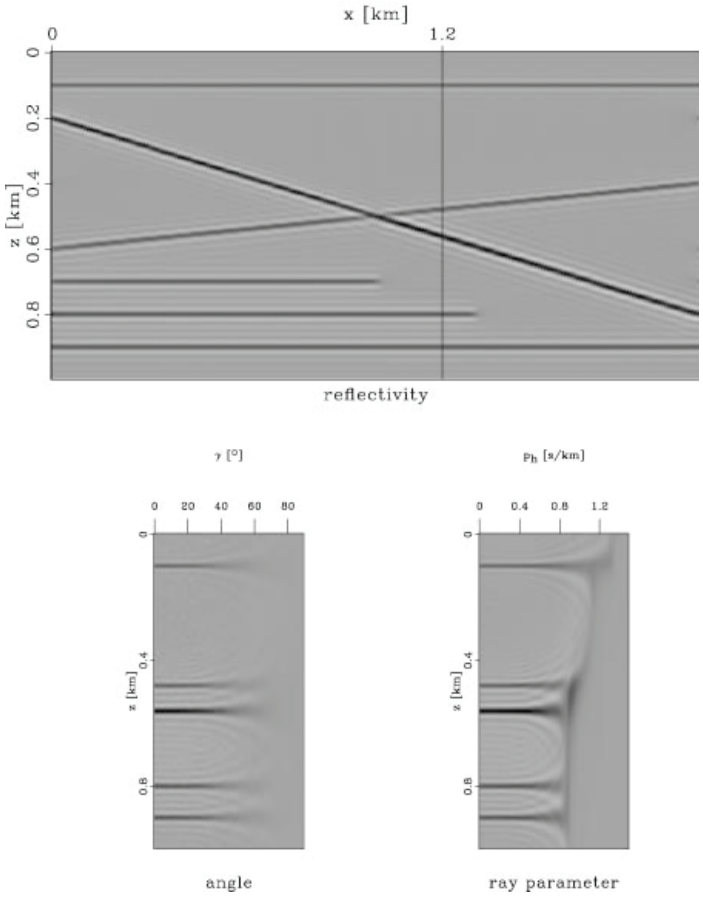

FIG. 12. Synthetic model imaged using the correct velocity model: section obtained by imaging at zero time and zero offset (top), angle-gather created in the image space (bottom left), and angle-gather created in the data space (bottom right) (Sava and Fomel, 2003).

4. FRACTURE DETECTION USING ANGLE-DOMAIN COMMON-IMAGE GATHERS

As mentioned throughout this paper, angle-domain common-image gathers have been widely employed in velocity analysis and AVO study. The application of ADCIGs in AVO study is known as amplitude versus angle and azimuth (AVAZ) technique in geophysical industry. Gray (2008) discusses that the AVAZ provides valid information about fractures at existing wells, in reservoir characterization specially in predicting the production rates of new wells, and in structural interpretation. Here is a brief summary to application of AVAZ in fracture study by Gray (2008).

The AVAZ method can be used to identify the presence of fractures between well locations using wide-azimuth 3D seismic data. The method is only capable of detecting the cumulative effect of swarms of aligned fractures and not individual fractures. In the mid 1990's, it began to be shown that there are measurable differences in the seismic AVO responses parallel and perpendicular to fractures, suggesting that AVAZ would be a viable technology. Gray (2008) examines some short case histories in which seismic AVAZ has been used in reservoirs where geologic information is available to check and calibrate the AVAZ response.

For Manderson Field, Gray (2008) showed that there is a good indicator, from outcrop, that the seismic AVAZ fracture analysis is detecting the correct orientation of the fractures. Also, the available core analyses were compared to the results derived from the AVAZ fracture analysis to confirm the AZAZ results. Also, he incorporates AVAZ attributes into reservoir characterization, which is extremely important because it allows for better determination of fracture information between the wells and thus a better understanding of fluid flow in the reservoir. The seismic AVAZ results provide a indirect measurement of the effects of fractures between the wells.

Based on the comparisons of AVAZ results to geologic indications of fractures (e.g. Gray et al, 2002), it seems that the seismic AVAZ attributes (crack density and fracture strike) do reflect the fracturing as understood from geologic studies of the same rocks and formations. In addition, the AVAZ attributes seem to provide important information on the distribution of fractures between the well locations. This information can be used to understand the reservoir, as at Manderson, and to help to predict production prior to drilling new wells.

Gray (2008) concluded the AVAZ results are consistent with core, outcrop, production, well logs and structural interpretations. Because the AVAZ records this fracture information between the wells, it adds significant information to the interpretation of fractured reservoirs that cannot be easily obtained in other ways.

5. CONCLUSIONS

The angle-domain CIG gathers have attractive properties when a complex velocity model causes multipathing of reflected energy. They are free of the imaging artefacts caused by reflector-position ambiguity that degrade the image obtained from either shot gathers or common-offset gathers. For acoustic case, the paper has reviewed two approaches in common-angle migration, namely an extension of classical Kirchhoff

method and wave-equation migration method. The 3D common (constant) opening angle M/I derived as integration over migration dip at an output point at depth. The derivation of common-opening angle Kirchhoff M/I follows the same classical lines as in previous Kirchhoff inversions, placing this method in the same class as earlier such inversions. Then this common-opening angle M/I in image point coordinates transformed to surface coordinate with a transformation that involves Jocobian for rays from image point to the source receiver point. Such integrals over source/receiver coordinates are more natural to implementation on seismic data.

The paper also reviewed two methods for extracting ADCIGs from the prestack wavefield downward-continued using wave-equation migration. In the data-space method angle gathers are evaluated using slant stacks of the downward-continued wavefield, prior to imaging; the data-space method produce angle-gathers as function of offset ray parameter, instead of true reflection angle. The second method, image-space method, computes angle gathers after imaging; this method does not involve the wavefields anymore, but the prestack images obtained by imaging at zero time. Image-space method directly produces angle-gathers as function of reflection angle.

ACKNOWLEDGEMENTS

We would like to thank CREWES industrial sponsors for funding my education. Also, I would like to thank Pat Daley for valuable discussions and being a source of information for me, and Rolf Maier for proof reading the text.

REFERENCES

Beydoun, W. B., Hanitzsch, C., and Jin, C., 1993, Why migration before AVO? A simple example, 55th mtg., Eur. Assn. Expl. Geophys., Extended Abstracts. B044.

Bleistein N., Cohen J. K., and Stockwell J. W., 2001 Mathematics of Multidimensional Seismic Imaging, Migration and Inversion (New York: Springer).

Bleistein, N., and Gray, S. H., 2002, A proposal for common-opening-angle migration/inversion *Center for Wave Phenomena Research Report* CWP-420.

Bleistein, N., Y., Zhang, S., Xu, S. H., Gray, and G., Zhang, 2005, Migration/inversion: Think image point coordinates, process in acquisition surface coordinates: Inverse Problems, **21**, 1715–1744.

Brandsberg-Dahl, S., de Hoop, M. V., and Ursin, B., 1999, Sensitivity transform in the common scattering-angle/azimuth domain: EAGE 61st Annual Conference, Expanded Abstracts.

Gray, D., Robert, G., Head, K. J., 2002, Recent advances in determination of fracture stike and crack density from p-wave seismic data, The Leading Edge ,*Soc. of Expl. Geophys., 21*, 3, 280-285.

Gray, D., 2008, Fracture Detection Using 3D Seismic Azimuthal AVO*,* CSEG RECORDER, March.

de Bruin, C., Wapenaar, C., and Berkhout, A., 1990, Angle-dependent reflectivity by means of prestack migration: Geophysics, **55**, 1223–1234.

de Hoop, M. V., Burridge,R., Spencer,C., and Miller,D., 1994,GRT/AVA migration/inversion in anisotropic media: SPIE—The Internat. Soc. for Optical Engineering: **23**, 15–27.

de Hoop, M. V., and S. Brandesberg-Dahl, 2000, Maslov asymptotic extension of generalized radon transform inversions in anisotropic elastic media: A least-squares approach: Inc=verse Problems, **16**, n0. 3, 519-562.

Duquet, B., 1996, Am´ eliarotion de l'imagerie sismique de structuresg´eologiques complexes: Ph.D. thesis, Universit ´e de Paris XIII.

Fomel S., 2004, Theory of 3-D angle gathers in wave-equation, 74th Ann. Internat.Mtg., Soc. Expl. Geophys., Expanded Abstracts, 1053.

Fomel S., Prucha, M., 1999, Angle-gather time migration, Stanford Exploration Project, Report 100, 141–151.

Mosher, C., and Foster, D., 2000, Common angle imaging conditions for prestack depth migration: 70th Ann. Internat. Mtg., Soc. Expl. Geophys., Expanded Abstracts, 830–833.

Nolan, C. J., and Symes, W. W., 1996, Imaging and conherency in complex structure: Proc. 66th Annual International Meeting, 359–363.
Prucha, M., Biondi, B., and Symes, W., 1999, Angle-domain common-image-gathers by wave-equation migration: 69th Ann. Internat.Mtg., Soc. Expl. Geophys., Expanded Abstracts, 824–827.
Sava, P. C., Fomel, S., 2003, Angle-domain common-image gathers by wavefiled continuation methods, Geophysics, **68**, 1065-1074.
Sollid A., Ursin, B., 2003, Scattering-angle migration of ocean-bottom seismic data in weakly anisotropic media, Geophysics, **68**, 641-655.
Stolk, C., and Symes, W., 2002, Artifacts in Kirchhoff common image gathers: 72nd Ann. Internat. Mtg., Soc. Expl. Geophys., Expanded Abstracts, 1129–1541.
Symes, W., 1993, A differential semblance criterion for inversion of multi-offset seismic reflection data: J. Geophys. Res,. **98**, 2061-2073.
Tura, A., Hanitzsch, C., and Calandra, H., 1998,3-D AVO migration/inversion of field data: The leading edge, **17**, 1578-1583.
Ursin, B., 2004, Parameter inversion and angle migration in anisotropic elastic media, Geophysics, **69**, 1125-1142.
Xu S., H., Chauris, G., Lambar´e, and N. S., Noble, 2001, Common-angle migration: A strategy for imaging complex media, Geophysics **66** 1877–94.
Zhang,Y., S., Xu, N., Bleistein, and G., Zhang, 2007, True-amplitude angle-domain, common-image gathers from one-way wave equation, Geophysics, **72**, S49-S58.

APPENDIX A: DERIVATION OF COMMON-ANGLE MIGRATION/INVERSION

The purpose of this appendix is to derive equation (1), reflectivity function, common-opening angle Kirchhoff M/I in image point coordinates. The start point is using Kirchhoff-approximated data. Kirchhoff-approximate data is an approximation of upward scattered field response from a single reflector. The Kirchhoff-approximate data to describe the recorded wavefield at receiver x_r due to a source at x_s:

$$u(x_s, x_r, w) \approx -iw \int_V \beta(x', \theta) A(x') \left|\nabla \tau(x')\right| e^{iw\tau(x')} dV \qquad \text{(A.1)}$$

with the volume integral to be carried out over the variable x'. In this equation

i. $\beta(x', \theta)$ is the subsurface point x' reflectivity function at the opening angle θ. Bleistein et al. (2001) describe the relation between β and the reflection coefficient $R(x, \theta)$ as: $\beta(x, \theta) = R(x, \theta)\dfrac{2\cos\theta}{c(x)}$.

ii. $\boldsymbol{\tau(x')}$ is the sum of the travel-times from the source and receiver, respectively, to the subsurface point x': $\tau(x') = \tau(x', x_s, x_r) = \tau(x_s, x') + \tau(x', x_r)$, with each of the separate travel-times being solutions of the eikonal equation.

iii. $\boldsymbol{A(x')}$ is a product of green's function amplitudes, $A(x') = A(x', x_s, x_r) = a(x_s, x')a(x', x_r)$, with the $\boldsymbol{a}$'s being a solution of the transport equation.

They proposed inversion formula as follow:

$$\beta(x,\theta) \sim \int_V iwW\, u(x_s, x_r, w)\; e^{-iw\tau(x)}\, dw\, d\alpha_1 d\alpha_2 d\varphi, \qquad \text{(A.2)}$$

with the kernel W is to be determined. In this equation, the α_1 , α_2 and azimuth φ are any parameters that define v (migration dip, see Figure 1). In this integral the x_s and x_r are determined from the position of point $\boldsymbol{x}$ with the ray directions determined by the choices of v, θ and φ. The W, x_s and x_r are considered as functions of the subsurface point x, migration dip v, opening angle θ, and the azimuth φ. The argument θ in the reflectivity, $\beta(x,\theta)$, is the prescribed opening angle of this common-angle inversion.

To learn about $\boldsymbol{W}$: substitute equation (A.1) for $\boldsymbol{u}$ into inversion formula (A.2), the result is

$$\beta(x,\theta) \sim \int_V \int\!\!\int w^2 W\, \beta(x',\theta) A(x') \left|\nabla\tau(x')\right| e^{iw[\tau(x')-\tau(x)]}\, d\alpha_1 d\alpha_2 d\varphi dw dV. \qquad \text{(A.3)}$$

Here the integral over the x' variable of the function $\beta(x',\theta)$ multiplied by a rather complicated weighting function produces the function $\beta(x,\theta)$. For this to occur, that complicated weighting function must be a Dirac delta function, at least asymptotically. Consequently, the integrand loses the oscillation that occurs for other choices of x' than x. In the language of asymptotic expansions of the integrals, the point $x' = x$ is a *critical point* of the integral. Therefore,

$$\delta(x'-x) \sim \int_V \int\!\!\int w^2 W\, A(x') \left|\nabla\tau(x')\right| e^{iw[\tau(x')-\tau(x)]}\, d\alpha_1 d\alpha_2 d\varphi dw dV. \qquad \text{(A.4)}$$

Approximating the integrand for x' in the neighborhood of x, the amplitude amounts to setting $x' = x$. Using a Taylor series expansion for the phase, function results in $w\left[\tau(x')-\tau(x)\right] \approx \mathrm{k}.(x'-x)$ with **k** is the wavenumber defined as

$$\boldsymbol{k} = w\nabla\tau(x')\,|_{x'=x} = w\nabla\tau \qquad \text{(A.5)}$$

Additionally, the gradient of the total travel time is in the direction of v (Figure 3),

$$\nabla\tau(x) = \frac{2\cos\theta}{c(x)}. \qquad \text{(A.6)}$$

Now the phase in equation (A.4) takes on the form familiar in Fourier transforms when expressed in terms of the new vector variable $\boldsymbol{k}$. Therefore, in equation (A.4) the integrations in the variables of v and w can replace by a volume integral in $\boldsymbol{k}$ as follows:

$$\delta(x'-x) \sim \iint_V w^2 W\, A\,(x)\left|\nabla\tau(x)\right| \left|\frac{\partial(w,\alpha_1,\alpha_2)}{\partial(k)}\right| e^{i\boldsymbol{k}.(x'-x)}\, d^3\boldsymbol{k}\, d\varphi \qquad \text{(A.7)}$$

Once the kernel $\boldsymbol{W}$ is determined, it is equation (A.3) that gives the common-angle M/I. In order to proceed, we need to know about the Jacobian appearing in equation (A.7). It is easier to calculate the inverse of this Jocobian. From equation (A.5),

$$\frac{\partial(\boldsymbol{k})}{\partial(w,\alpha_1,\alpha_2)} = w^2 h(x,v,\theta), \qquad \text{(A.8)}$$

with

$$h(x,v,\theta) = \det\begin{bmatrix} \nabla\tau(x,v,\theta) \\ \dfrac{\partial\nabla\tau}{\partial\alpha_1}(x,v,\theta) \\ \dfrac{\partial\nabla\tau}{\partial\alpha_2}(x,v,\theta) \end{bmatrix}. \qquad \text{(A.9)}$$

That is, $h(x,v,\theta)$ the so called Beylkin determinant is now in the variables of integration of the migration dip. The Beylkin determinant is substituted into equation (A.7) to obtain

$$\delta\left(x'-x\right) \sim \iint_V w^2 W \frac{A\,(x)\left|\nabla\tau(x)\right|}{\left|h(x,v,\theta)\right|} e^{i\boldsymbol{k}.(x'-x)}\, d^3\boldsymbol{k}\, d\varphi \qquad \text{(A.10)}$$

Comparing this result with the exact delta function,

$$\delta(x'-x) = \frac{1}{8\pi^3}\int e^{i\boldsymbol{k}.(x'-x)}\, d^3\boldsymbol{k}\ , \qquad \text{(A.11)}$$

the kernel $\boldsymbol{W}$ is to choose so that

$$W(x,v,\theta,\varphi)\frac{A\,(x)\left|\nabla\tau(x)\right|}{\left|h(x,v,\theta)\right|} = \frac{1}{8\pi^3} \qquad \text{(A.12)}$$

or

$$W(x,v,\theta,\varphi) = \frac{\left|h(x,v,\theta)\right|}{8\pi^3 A\,(x)\left|\nabla\tau(x)\right|}\ . \qquad \text{(A.13)}$$

Now the Beylkin determinate, equation (A.9), using $\nabla\tau$ from equation (A.6) becomes

$$h(x,v,\theta)=\left[\frac{2\cos\theta}{c(x)}\right]^3 det\begin{bmatrix} v \\ \frac{\partial v}{\partial \alpha_1} \\ \frac{\partial v}{\partial \alpha_2}\end{bmatrix}=\left[\frac{2\cos\theta}{c(x)}\right]^3 v.\frac{\partial v}{\partial \alpha_1}\times\frac{\partial v}{\partial \alpha_2}\ . \qquad \text{(A.14)}$$

Now using equation (A.6) for $|\nabla\tau|$, condition *iii* for *A(x)* and this last result for $h(x,v,\theta)$ substituted in equation (A.2) for $\beta(x,\theta)$, one obtains

$$\beta(x,\theta)=\frac{1}{4\pi^2}\left[\frac{2\cos\theta}{c(x)}\right]^2\int\frac{D(x,x_s,x_r)}{A(x,x_s)A(x,x_r)}\left|v.\frac{\partial v}{\partial \alpha_1}\times\frac{\partial v}{\partial \alpha_2}\right|d\alpha_1 d\alpha_2 d\varphi, \qquad \text{(A.15)}$$

the quantity ***D*** is a filtered version of input traces written as

$$D\left(x,x_s,x_r\right)=\frac{1}{2\pi}\int iwu(x_s,x_r,w)e^{-iw\tau(x)}\,dw. \qquad \text{(A.16)}$$

For fixed value of azimuth φ, the inversion formula becomes

$$\beta(x,\theta,\varphi)=\frac{1}{4\pi^2}\left[\frac{2\cos\theta}{c(x)}\right]^2\int\frac{D(x,x_s,x_r)}{A(x,x_s)A(x,x_r)}\left|v.\frac{\partial v}{\partial \alpha_1}\times\frac{\partial v}{\partial \alpha_2}\right|d\alpha_1 d\alpha_2. \qquad \text{(A.17)}$$

Considering (i) the reflectivity function would be:

$$\beta(x,\theta,\varphi)=\frac{1}{4\pi^2}\frac{2\cos\theta}{c(x)}\int\frac{D(x,x_s,x_r)}{A(x,x_s)A(x,x_r)}\left|v.\frac{\partial v}{\partial \alpha_1}\times\frac{\partial v}{\partial \alpha_2}\right|d\alpha_1 d\alpha_2\ . \qquad \text{(A.18)}$$

Going further, it is needed to define the parameters α_1 and α_2, with which the vector *v* is defined; as the vector *v* is the integration variables in inversion formula, then the inversion operator can be also defined. The polar coordinates are the most straightforward choice, in terms of these coordinates

$$v=(\sin\alpha_1\cos\alpha_2,\sin\alpha_1\sin\alpha_2,\cos\alpha_1)$$

carrying out the differentiations in equation (A.14), the Beylkin determinant will be

$$h(x,v,\theta)=\left[\frac{2\cos\theta}{c(x)}\right]^3\sin\alpha_1. \qquad \text{(A.19)}$$

For the choice of polar coordinate α_1 and α_2, then the final formula for inversion will be

$$R(x,\theta,\varphi)=\frac{1}{4\pi^2}\frac{2\cos\theta}{c(x)}\int\frac{D(x,x_s,x_r)}{A(x,x_s)A(x,x_r)}\sin\alpha_1 d\alpha_1 d\alpha_2. \qquad \text{(A.20)}$$